remote sensing

MDPI

Article

Laser Scanning Investigation and Geophysical Monitoring to Characterise Cultural Heritage Current State and Threat by Traffic-Induce Vibrations: The Villa Farnesina in Rome

Antonio Costanzo [1,*], Sergio Falcone [1], Carmelo La Piana [1], Virginia Lapenta [2], Massimo Musacchio [1], Antonio Sgamellotti [2] and Maria Fabrizia Buongiorno [1]

[1] Istituto Nazionale di Geofisica e Vulcanologia, 00143 Rome, Italy
[2] Accademia Nazionale dei Lincei, 00143 Rome, Italy
* Correspondence: antonio.costanzo@ingv.it

Abstract: A multidisciplinary approach is often the only way to assess the state of the cultural heritage, thus involving different specialist expertise and techniques. The paper shows the paired use of terrestrial laser scanning (TLS) and geophysical monitoring (GM) to detect past effects and analyse the actual vibration levels induced by traffic on cultural heritage. The case study is the Villa Farnesina, one of the most important Renaissance buildings commissioned by the banker Agostino Chigi. The Villa contains frescoes attributed to Raphael and other famous 16th century artists, and it is located a few meters from the Lungotevere, which is one of the busiest roads in the historic centre of Rome. Testimonies report the damages caused by the construction of the embankment of the Tiber River, as well as by the traffic in the second half of the 20th century, so much so as to require requalification of the road artery. The TLS survey allows for detecting cracks and deteriorations of the frescoes, although these were subjected to restoration activities over the time, whereas the (GM) allows analysing actual vibrations induced by traffic at the different floors and outside the Villa. Although the measured vibration limits, as velocity peaks in defined frequency ranges, are below the thresholds established by international codes, the importance of the wall paintings and their already-shown susceptibility to damage suggest keeping the building under constant monitoring.

Keywords: terrestrial laser scanning; geophysical monitoring; cultural heritage; traffic-induced vibrations; Raphael's frescoes; Villa Farnesina; Lodge of Galatea

Citation: Costanzo, A.; Falcone, S.; Piana, C.L.; Lapenta, V.; Musacchio, M.; Sgamellotti, A.; Buongiorno, M.F. Laser Scanning Investigation and Geophysical Monitoring to Characterise Cultural Heritage Current State and Threat by Traffic-Induce Vibrations: The Villa Farnesina in Rome. *Remote Sens.* **2022**, *14*, 5818. https://doi.org/10.3390/rs14225818

Academic Editor: Fulong Chen

Received: 6 October 2022
Accepted: 14 November 2022
Published: 17 November 2022

1. Introduction

The urban transport is one of the crucial issues to guarantee the urban sustainability of cities in the mid- and long-term. The main challenge is to find solutions to address peculiar problems related to the mobility of people and freights, such as reasonable travel times, the technical and economic feasibility of the infrastructure and sustainable integration with the urban fabric [1]. Another important issue to be addressed, however, is that relating to the mitigation of the negative effects due to the transport infrastructures on the life quality of citizens and tourists, such as the polluting impact on the environmental matrix [2–4] as well as the physical one on the built heritage [5–7]. The exposure generally increases when the assets are in populated urban centres seamlessly; indeed, in many cities throughout the world, the proximity of busy transport infrastructure represents a threat both to the environment and built heritage. In the latter component of the urban environment, the historical centres, ancient buildings and archaeological sites are often the most exposed assets; in fact, these show a high vulnerability both to events of rapid onset and of typically short duration (e.g., dynamic loads due to earthquakes) [8–12] and those of slow onset and typically protracted duration (e.g., continuous, cyclic transient and mixed vibrations due to anthropic activities) [13–16].

Vibrations from human sources, and in particular those induced by heavy traffic flows (due to vehicles, subways, railways, etc.), are among the most common causes of small aesthetic damages to structures [13,14,17–19]; moreover, they can cause loss of integrity and increased vulnerability of the assets of cultural heritage. In fact, although the traffic-induced vibrations are generally characterised by low amplitude, their high number of loading cycles over time can have particularly negative effects on the historic masonry due to its inability to accommodate tensile stresses, with the consequent deterioration of mortar and plasters and the detachment of the masonry unit, which can result in a progressive reduction of the resistance for the entire structure [20,21].

However, the dynamic behaviour of the pavement–soil system is generally too complex to be analysed because it is characterised by a vibration regime that is the superposition of effects related to both body and surface waves propagating in a heterogeneous field [13]. In addition, the structures alter the frequency content and amplitude of the ground motion generated by the vibration source because of the resonance phenomena connected with their dynamic properties. In this context, the amplification phenomena might play a relevant role, leading to high stresses in both structural and non-structural elements. Thus, the non-structural aesthetic elements of the cultural heritage assets, such as plasters, frescoes, and decorative parts, which are generally made of fragile materials with low-tensile strengths, are the most exposed.

Therefore, in addition to characterising the levels of vibration produced, it is also extremely important to support knowledge of cultural heritage in order to assess the current vulnerability; this is another important factor in the threat analysis (cf. [17–23])

Vibration monitoring is widely adopted in civil engineering to assess the behaviour of the structures under ambient noise due to natural excitations or human sources. The vibration monitoring system is mainly based on contact sensors or remote sensing technologies [24–28].

Moreover, international standards provide threshold values of the vibrations [29–31]—expressed as Peak Particle Velocity (PPV) or Peak Particle Component Velocity (PCPV)—as a function of the dominant frequency range. These values should not be exceeded to avoid damage to buildings under preservation (cf. Table 1). It is worth pointing out that the codes generally provide two types of vibration: short-term (or transient) and long-term (or continuous). The latter ones are generally connected to fatigue damage.

Table 1. Thresholds for vibrations from International Standards.

Frequency Range	PPV/PCPV	Threshold Values (mm/s)	Exposition	Component	
1–10 Hz	PCPV +	3	short-term	horizontal	DIN 4150-3 [29]
10–50 Hz	PCPV +	3–8		horizontal	
50–100 Hz	PCPV +	8–10		horizontal	
All	PCPV *	8		horizontal	UNI 9916 [30]
All	PCPV +	2.5		horizontal	
All	PCPV +	20		vertical	
All	PCPV +	2.5	long-term	horizontal	
All	PCPV +	10	short-term	vertical	
8–30 Hz	PPV	7.5–15	occasional	module of resultant vector	SN 640312 [31]
30–60 Hz	PPV	10–20			
60–150 Hz	PPV	15–30			
8–30 Hz	PPV	3–6	frequent		
30–60 Hz	PPV	4–8			
60–150 Hz	PPV	6–12			
8–30 Hz	PPV	1.5–3	continuous		
30–60 Hz	PPV	2–4			
60–150 Hz	PPV	3–6			

+ At the foundation; * At horizontal plane of highest floor.

In this context, the city of Rome is an interesting field of study to analyse the effects of traffic-induced vibrations on cultural heritage, due to the high concentration of archaeological assets and buildings of high historical value in the urban area. Just think that the entire historic centre is a UNESCO World Heritage Site [32]. At the same time, historic centres and neighbourhoods are densely populated, and therefore they are required to be served by important infrastructures to ensure the mobility of people and wares. Within the urban area, a peculiar case study is represented by Villa Farnesina (Figure 1): one of the most important buildings of the Italian Renaissance. Today, the garden of Villa Farnesina is bordered on one side by Lungara Road and on the other by Lungotevere Road, running along the Tiber River and being one of the most important arteries within the historic centre. In the twentieth century, the Villa suffered extensive damage due to the vibrations generated by traffic on the Lungotevere, so that several restoration interventions of the frescoes were necessary, as well as road improvements to reduce the impact on the historic building [33]. Moreover, an experimental investigation with impact tests was carried out by ENEA over 20 years ago [14] to analyse the anti-vibration effects due to the intervention on the road pavement. Furthermore, very short recordings of traffic-induced vibrations were performed by the same authors only on the road and at the base of the building.

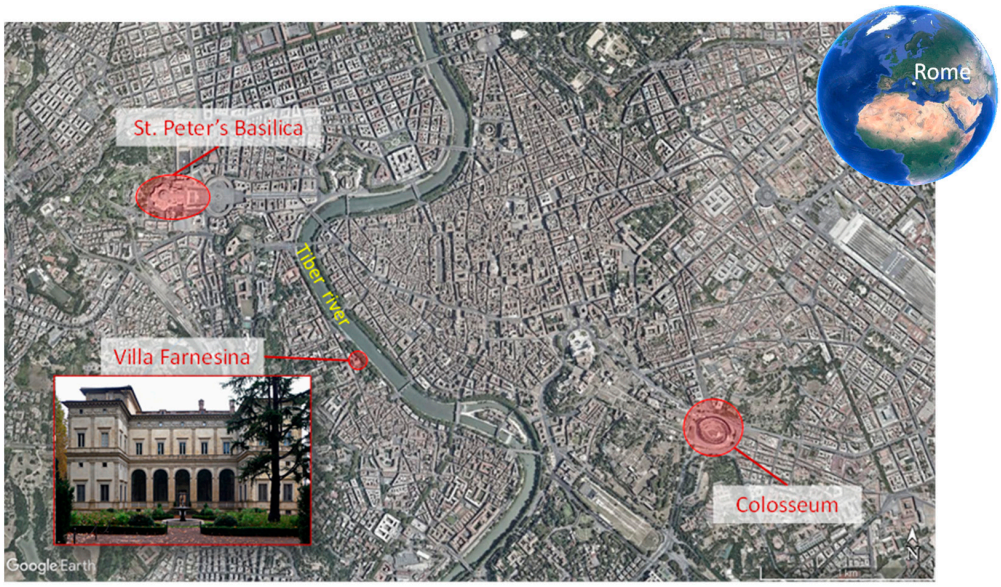

Figure 1. The location of the Villa Farnesina in the historic centre of Rome and with respect to the Tiber River, the Colosseum and St. Peter's Basilica, also indicated as reference elements (picture modified by Google Earth®).

Given the partnership between the Istituto Nazionale di Geofisica e Vulcanologia (INGV) and the Accademia dei Linceii that is the owner of Villa Farnesina, within the Dynamic Planet project [34], a temporary monitoring system inside and outside the Villa Farnesina was performed with the main objectives: (1) to contribute to the analysis of the health state of frescoes in the Lodge of Galatea by means of terrestrial laser scanning and (2) to evaluate the vibrations at the different levels of the building mainly due to the current traffic flows on the two roads. Preliminary results only regarding the monitoring of the vibrations were presented by the same authors in an international conference [35].

The proposed method tries to support the evaluation of both fundamental factors, characterising the threat due to the loads induced by anthropic activities on cultural heritage, including the level of the vibrations and the vulnerability of the assets themselves.

2. Materials and Methods

2.1. The Case Study: Villa Farnesina

The Renaissance Villa of the banker Agostino Chigi, one of the richest men in Europe in the sixteenth century, was later called Villa Farnesina when it became the property of the Farnese family. The Villa was designed by the Sienese Baldassare Peruzzi and frescoed by artists of the calibre of Raphael, Sebastiano del Piombo, Sodoma, and Peruzzi himself, thus representing one of the highest expressions of the Italian Renaissance. It soon became a model throughout Europe also for its peculiar characteristics as a suburban Villa, surrounded by gardens rich in exotic plants, acting as a "hortus conclusus" (secret garden). Due to the Tiber River, which laps it, the Villa has undergone several modifications over the centuries; the famous Lodges of Cupid and Psyche and of Galatea, located on the ground floor, have been closed to remove the frescoes from adverse weather conditions and flooding of the Tiber.

Following the 17 m high flood in Rome on 28 December 1870, a special commission took charge of the choices of the intervention by approving a project commissioned by Giuseppe Garibaldi in 1875. Work included the regularisation of the riverbed at 100 m and the construction of the embankments of the Tiber, called walls, as well as demolishing the pre-existing buildings on the riverbank and a large part of the gardens to the north of the Villa Farnesina. These interventions, which began in 1875, ended in 1925 when several bridges were built that connected the two banks of the river and open roads, with a wide flow, known as Lungotevere.

The construction of the walls already put a strain on the resilience of the building, so much so that the Duke of Ripalta, owner of the Villa in the nineteenth century, managed to replace the pile drivers for the construction of the foundations with compressed air to prevent the strong vibrations from causing detachment of the frescoed plasters.

Towards 1950, what the Duke of Ripalta had feared materialised: with the increase of heavy motorised traffic on the stretch of the Lungotevere adjacent to the Villa Farnesina, an accentuation of damage began to manifest in the shapes of the peppers that decorate the exterior of the building and in the frescoed plasters that decorate the interior. The intensity of both surface and underground vibrations was compared to an earthquake of the 4th–5th degree on the Mercalli scale. In the autumn of 1953, the large lesion in the vault of the Lodge of Galatea reopened and three corbels of peppers were detached from the external cornice. The Accademia dei Lincei decided on the restoration and authorised the Conservator, Eng. Giovanni Massari, to collect, with scientific observations, all the data necessary to control the phenomenon of damage that had widely occurred in the plaster of the building.

From 1953 to 1956, by means of oscillographs, three detection campaigns were organised to reveal the vibrations which reached the Farnesina both at the level of the garden and at a depth of three metres at the level of the foundations. In 1956, having had all the results of the investigations available, a commission of specialists was appointed by the Accademia dei Lincei chaired by Prof. Eng. Gustavo Colonnetti, Associate of the Academy and former President of the Research Council with the task of studying the defence plan of the Farnesina.

In June 1959, after three years of work, Eng. Colonnetti handed the final report of the Commission over to the President of the Academy, prof. Francesco Giordani.

The elementary solutions of an elastic belt inserted between the footpaths and the plinth and the other of a cavity around the building were discarded since they would not have had an intercepting effect with respect to the foundation. The presence of an aquifer is just 90 cm below the basement floor was also discarded, as was the hypothesis of a possible deepening of the cavity until it was effective.

The studies then focused on the possible modification of the road surface structure to make it capable of absorbing the accelerations as they arise, even more so when it was found that this modification could be limited to 50 or 60 metres, at most, in the length of that stretch of the Lungotevere, which the oscillograms indicated as the most highly

dangerous area. The goal to be achieved was set in this form: "to create an intercepting structure at street level that prevents the wave from descending within the embankment of the Lungotevere, and to avoid any amplification due to waves reflected by the wall on the Tiber" [36]. This intercepting structure took the form of an oscillating complex consisting of the mass of a new road surface resting on elastic elements, "a floating plate" which was intended to reduce the residual amplitude of vibrations to one fifth, a limit which is totally compatible with the conservation of the frescoes.

The durability of rubber was also discussed during the Commission's studies. Given that the pads would have been completely removed by the sun's ultraviolet rays as well as from the action of oils and fats, and given the specific qualities of the blend used by the Pirelli Saga, full confidence in the practically unlimited duration of the chosen device was confirmed.

For eleven years from 1959 to 1970, the Colonnetti project oscillated from one to the other of the various administrations involved while the detachment of the frescoed plasters progressed to such an extent that prof. Pasquale Rotondi, Director of the Central Institute of Restoration, had to have a large nylon net applied under the vault of the Lodge of Galatea to collect the pieces of plaster that were beginning to fall.

The works began in August 1970 thanks to the intervention of the Municipality of Rome and ended in mid-December, in just four months.

The structure reaches a depth of 1.65 m and extends in length along the road axis for 64.52 m with a width of 13.50 m. The carriageway was divided along the axis of the road into two independent halves, each of which is an oscillating monolithic block weighing about 400 tons, resting on just over 1000 rubber pads. At the two heads, to avoid the jolt of the vehicles where the new elastic structure meets the old static ballast, a common bridge joint 2 metres long was inserted. This was a sturdy reinforced concrete plate connected on one side with a hinge to the elastic structure oscillating and, on the other hand, matching the old roadbed through a bitumen cushion [33].

This was the first case in Europe (and beyond) of renovating a road to safeguard a monument damaged by today's heavy traffic.

Both for the alluvial nature of the foundation soil and for the construction of the riverbanks (and for the consequent raising of the aquifer), the building still continues to undergo, in its various parts, progressive micro-deformations; as a result of this, inevitably, micro-cracks are produced both on the paintings and in the walls.

2.2. Methodology

Figure 2 shows a scheme of the methodology used for the survey techniques adopted in this work, with indication of the intermediate products and expected outcomes, which were both to detect anomalies on the surfaces of the assets, through terrestrial laser scanning, and to assess the vibration levels, by means of a temporary geophysical monitoring.

2.2.1. Laser Scanning Survey

The laser scanning surveys were executed to produce a 3D digital model of the vault of the Lodge of Galatea, in order to assess any signs on the frescoes due to the vibrations of the structure. Indeed, this architectonic element seems to have been the most damaged because of the vibrations from the traffic on the Lungotevere [33]. Therefore, in this first survey, particular attention was paid to monitoring this Lodge, which hosts the famous fresco "Triumph of Galatea" attributed to Raphael on a wall, as well as other frescoes just as important on the vault.

This survey was performed through a Z+F Imager® 5010c laser scanner (Zoller & Fröhlich, Wangen im Allgäu, Germany), with the measurement method based on phase comparison (e.g., [37,38]) of a wavelength of 1.5 µm. The laser scanner sensor can be used on close range up to 187 m, acquiring over a million points per second, with measurement accuracies beneath 1 mm for a distance of a few metres. Moreover, a high dynamic range (HDR) camera is also mounted on the Z+F Imager® 5010c [39], so that the instrument is

capable of generating panoramic pictures with 80 Mpixel resolution for colourising the point clouds. Therefore, the laser scanner allows acquiring geometrical position, intensity, and colour, at the same time, thus permitting the analysis of both images and geometry in order to detect any anomalies on the surface [40–42].

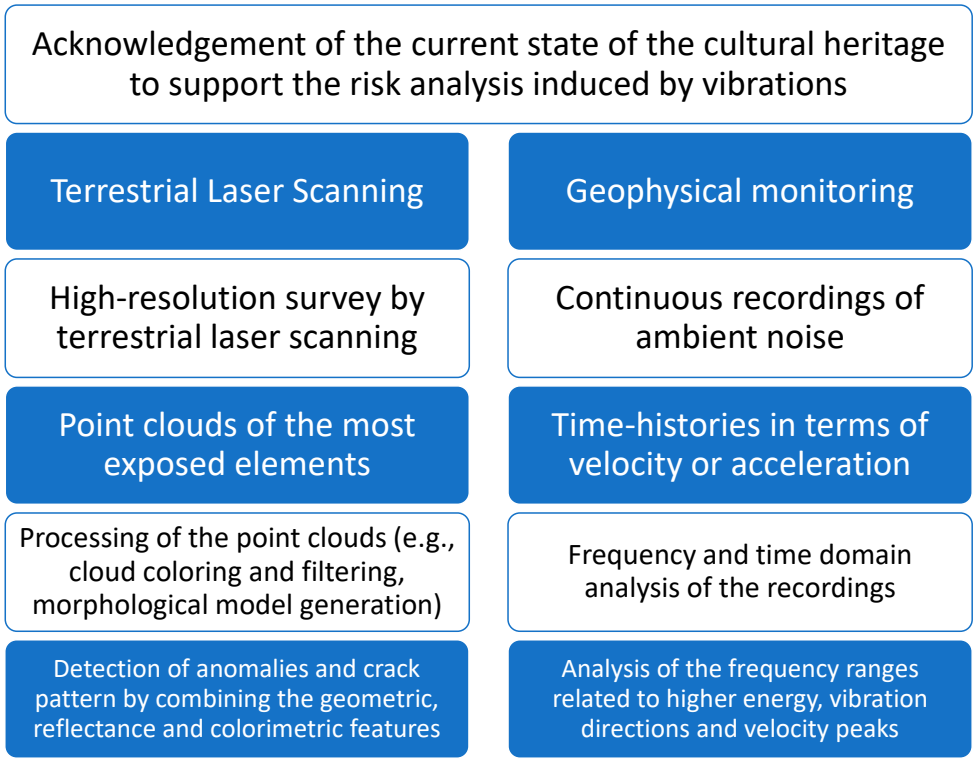

Figure 2. Scheme of the techniques adopted with intermediate products and main outcomes.

Six scans were performed with a "super high resolution" of the instrument (20,000 pixel/360°), within the same day to cover all parts of the vault without hidden zones. The scans were pre-processed to remove noise by setting distance range (0.4–100m), reflectance range (0.05–1.00) and the mixed point filter. Afterwards, all the scans were pre-aligned scan-to-scan with the point pairs, i.e., selecting at least 3 common points in the reference scan and in the other one free to rotate and translate. A mean registration error of less than 2 mm was ensured between scan pairs. At the end of this stage, a bundle adjustment algorithm was applied to all scans to align all the scans together to obtain a complete 3D model with a mean error of about 1.46mm. The processing of filtering and alignment was performed by using the JRC 3D Reconstructor software "https://www.gexel.it/it/software/reconstructor" (accessed on 15 November 2022).

Figure 3 shows the vault through the arrangement of all point clouds. However, the point clouds were analysed singularly, as seen the results reported in the figures shown in the next section, in order to both avoid introducing errors due to their alignment and effects on the images due to the variability of the natural light conditions.

The single point clouds were processed to obtain:

- The RGB Colour information by combining the high-resolution pictures with the point cloud by mean of the Z+F LaserControl® [43];
- The local morphology by calculating, for each point, the normal direction to the plane, obtained by interpolating all the points within a distance of 2 cm from the reference one through a script implemented in Cloud Compare [44];
- The "false" colours, enhanced by combining the "true" ones with the intensity of laser signal (at higher spatial resolution) using pan-sharpening techniques. This processing was performed through an algorithm implemented in Cloud Compare based on

Brovey transformation (cf. [45]), that allows obtaining false R'G'B' components by dividing the true RGB components by their sum and then multiplying them by the scalar intensity, normalised in the range 0–255.

Figure 3. 3D reconstruction of the Lodge of Galatea through the alignment of six point clouds.

2.2.2. Geophysical Monitoring

During the period between October 2020 and March 2021, a temporary seismic network was installed within the historic building. The main objective was the continuous recording of ambient noise, in order to assess the level of the vibrations in the different parts of the structure. Moreover, given that the two roads are the main sources of noise, and the Lungotevere Road is between the most relevant thoroughfares crossing the historic centre of the city, two other recording stations were located in the garden on the sides of the Villa closer to the roads.

Therefore, the network was comprised ten seismic stations: two in the garden at the ground level on the Lungotevere side (T1184 in Figure 4) and on the opposite one near the Lungara road (T1186 in Figure 4); two on the basement floor, also here on both sides (T1192 and T1189 in Figure 4); (iii) three on the first floor (T1191, T1181, T1188 in Figure 4); three on the second floor (T1190, T1182, T1185 in Figure 4).

To analyse how the waves propagate on the different levels of the building, three stations were placed along the vertical axis that crosses the Lodge: in the basement (T1192), on the floor (T1191) and above the vault (T1190), in addition to one installed in the garden on the same side (T1184). The other sensors were placed in correspondence to the Lodge of Cupid and Psyche and on the opposite side of the Villa, in order to assess how the vibrations decrease moving away from the main source.

The stations were composed of CENTAUR digitisers [46], each equipped with a TRILLIUM broadband seismometer [47] and TITAN accelerometer [48]. Time histories were recorded in the three orthogonal directions oriented along the north–south, east–west, and up–down directions and the data were sampled at 500 Hz using 24-bit analogic-to-digital converters. The embedded GPS system at each station assures time synchronism. A local wireless network was implemented for the data transmission thanks to a set of antennas, which allowed us to connect the stations to the internet line, made available by the Accademia dei Lincei. In this way, the recordings by the seismic stations were

transmitted in real-time to the server located in the Cultural Heritage Laboratory of the INGV headquarter of Rende.

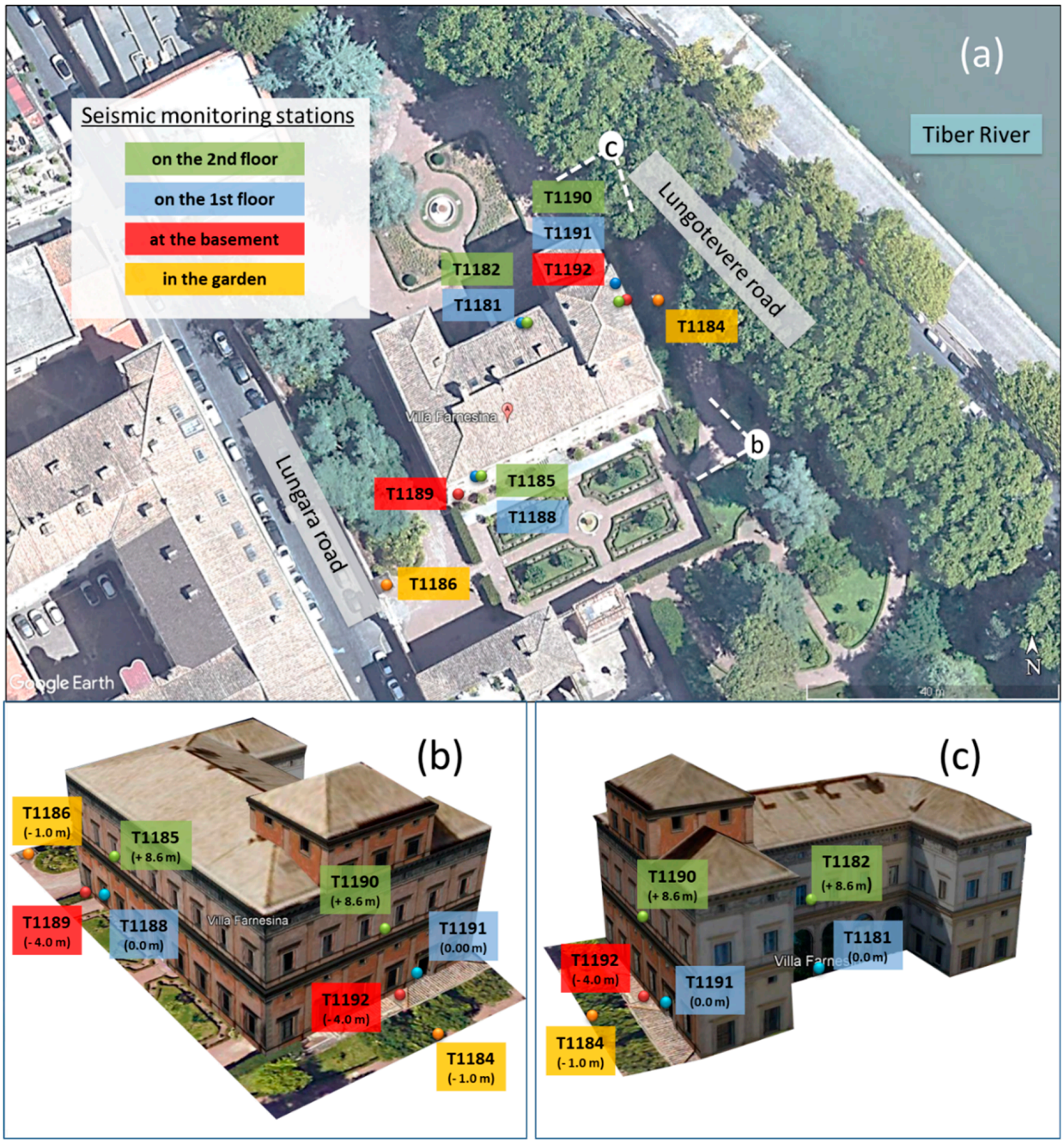

Figure 4. Villa Farnesina with respect to the Lungotevere Road and the Tiber River (by Google Earth ©). (**a**) 3D views; (**b**,**c**) Arrangement of the seismic network with stations at the various levels.

To analyse the characteristics of the whole dataset, statistical analyses were performed in the frequency domain by means of the Power Spectral Density (PSD). The calculation was performed on floating windows on the recorded signal of duration 3600 s. Therefore, on each window, a taper (with a 10% cosine taper function) is applied to the signal to attenuate the effect of spectral leakage, then the Discrete Fourier Transform (DFFT) is calculated,

The finite-range Fourier transform of a periodic time series y(t) is given by

$$Y(f, T_r) = \int_0^{T_r} y(t) e^{-i2\pi ft} dt \quad (1)$$

where T_r is the length of the analysed time series and f is the frequency.

For discrete frequency values, f_k, the Fourier components are defined as

$$Y_k = \frac{Y(f_k, T_r)}{\Delta t} \quad (2)$$

for

$$f_k = \frac{k}{N\Delta t} \quad (3)$$

where Δt is the sample interval and N is the number of samples in each time segment, therefore

$$N = \frac{T_r}{\Delta t} \quad (4)$$

Hence, using the Fourier components as defined, the total PSD estimate is defined as

$$P_k = \frac{2\Delta t}{N} |Y_k|^2 \quad (5)$$

The PSD for each of the analysis windows is obtained through the square modulus of the amplitude spectrum obtained with the DFFT, multiplied by a shape normalisation factor [49]. Finally, the instrument sensor response is removed by deconvolution in the frequency domain.

The monitoring time allows for disposing a large collection of signals from the entire observation period; therefore, it permits us to calculate PSDs over time, thus obtaining the Probability Density Function (PDF) by using the PQLX code [49,50]. In fact, the PDF describes the probability distribution of the spectral ordinates of the PSD as a function of the frequency, representing a statistic of the vibration levels at each recording site. Figure 5 shows the PDFs from the recordings acquired by the seismic stations in the garden and in the basement. In addition, the curves relating to the New High Noise Model (NHNM) and the New Low Noise Model (NLNM) were used as references of the noise values, representing, respectively, the upper and lower limits of the global noise model proposed by Peterson [51]. It is worth noting that noise levels assume maximum values in the garden at frequencies greater than 10 Hz and, especially, on the horizontal components. Instead, Figures 6 and 7 report the PDFs on the 1st and 2nd floor of the Villa Farnesina, respectively. The noise levels seem to increase moving from the Lungara side to the Lungotevere side at high frequencies, especially in correspondence with the 1st floor. Moreover, vibrations around 2 Hz assume values practically comparable with those at high frequencies, in correspondence with the 2nd floor.

The statistical analysis of the data does not seem to indicate significant differences between the vibration regimes, observable in some specific periods of the whole observation time, but rather between daytime and night-time hours throughout the day, as shown in the next section. However, a specific analysis, for example, to evaluate the possible lowering of the vibration level during the lockdown days was not a specific objective of this work, also because in that period heavy vehicles and cars continued to circulate to guarantee deliveries and to allow people to stock up on essential goods.

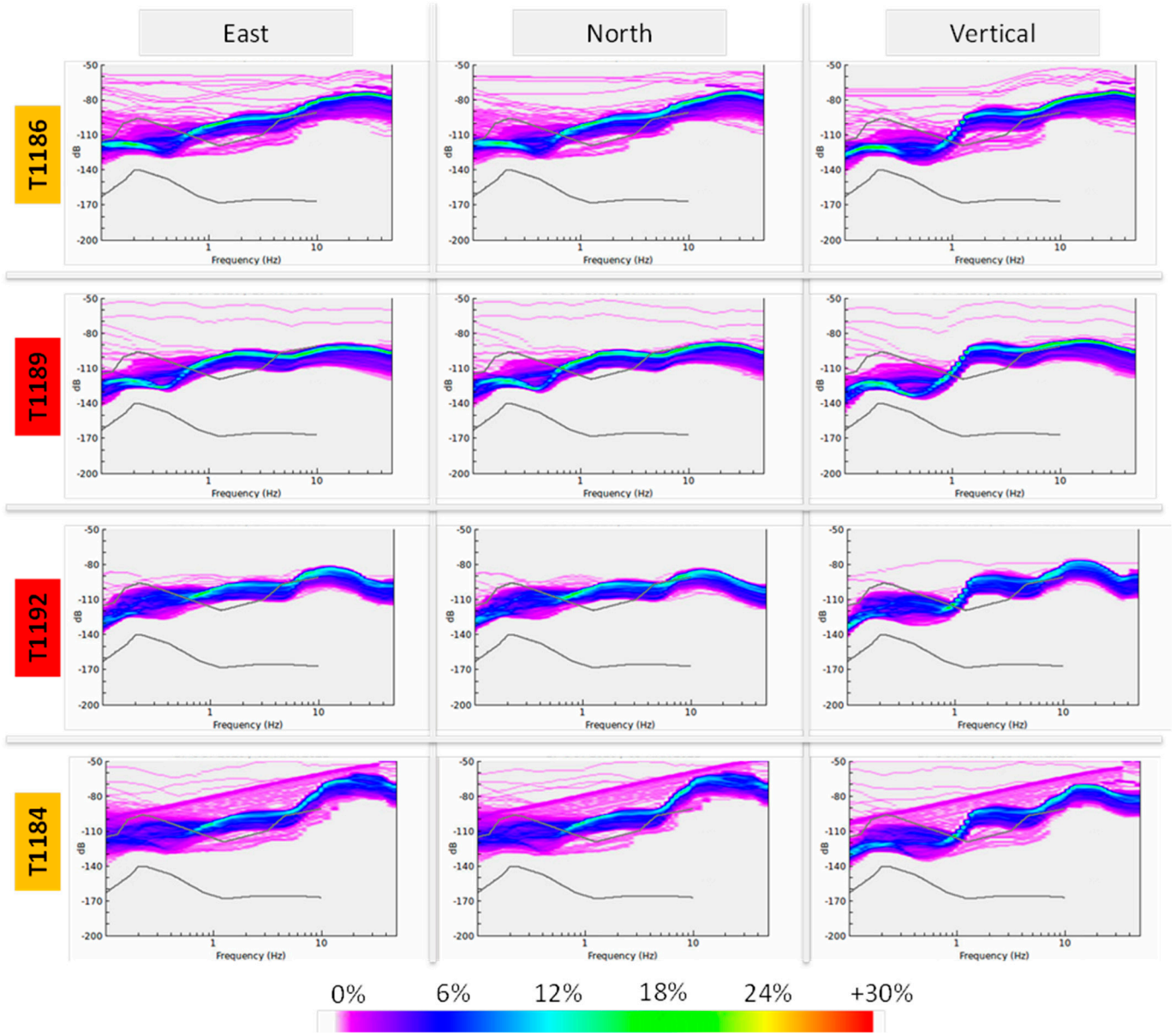

Figure 5. Probability Density Function (PDF) of Power Spectral Densities (PSD) expressed as dB over the frequency range 0.1–50 Hz for the recording sites at the basement (red) and in the garden (orange). The PDFs are reported for the three recording directions: east–west, north–south and vertical.

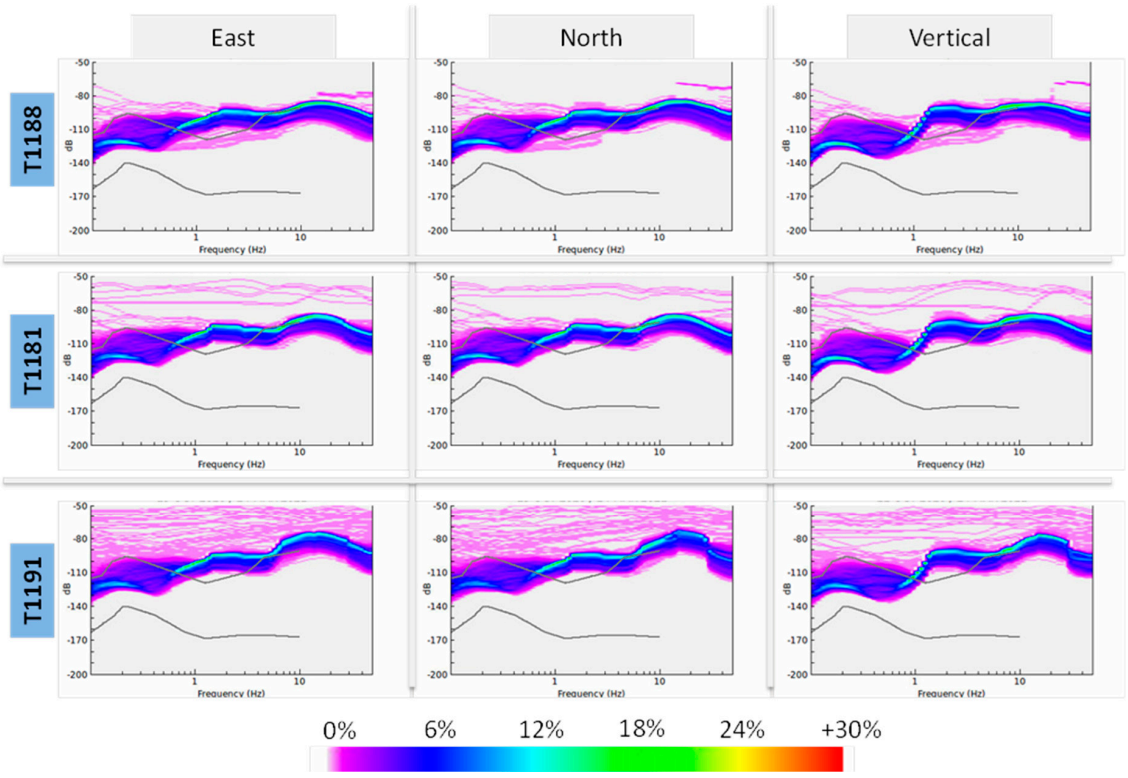

Figure 6. Probability Density Function (PDF) of Power Spectral Densities (PSD) expressed in dB over the frequency range 0.1–50 Hz for the 1st floor of the building. The PDFs are reported for the three recording directions: east–west, north–south and vertical.

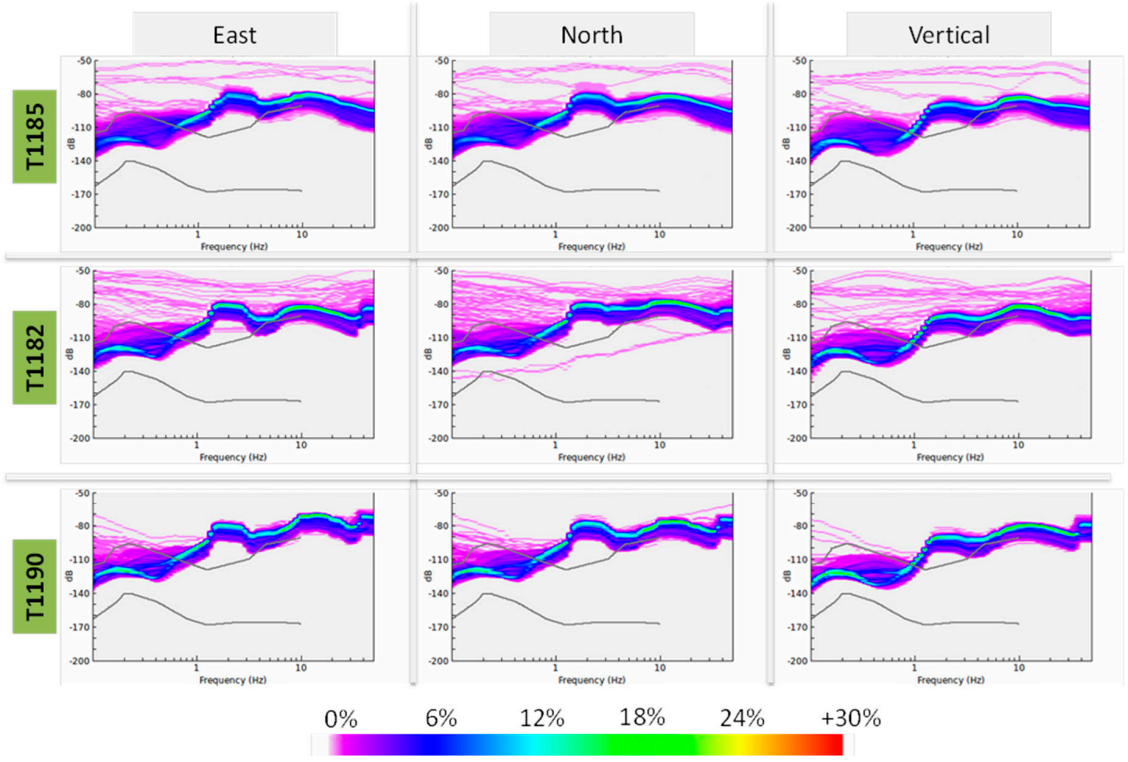

Figure 7. Probability Density Function (PDF) of Power Spectral Densities (PSD expressed in dB over the frequency range 0.1–50 Hz for the 2nd floor of the building. The PDFs are reported for the three recording directions: east–west, north–south and vertical.

3. Results

3.1. The Signs of the "Past" on the Frescoes

The 3D model of the Lodge of Galatea allows for the detection of crack signs and alteration in the plaster on the entire vault. By analysing the two frescoes, which feature Elice (Figure 8) and Perseus and Medusa (Figure 9) and cover a large part of the upper area of the vault, these signs are difficulty detectable with the naked eye or through non-professional pictures, as well as by the 3D-coloured model (cf. Figures 8a and 9a). Instead, cracks and alterations become more evident when the same model is enhanced by means of composition of the information both on the colours and intensity (cf. Figures 8b and 9b). Moreover, these findings were also found for the model representing local morphology (cf. Figures 8c and 9c).

Figure 8. Fresco of Elice on the vault of the Lodge of Galatea investigated through laser scanning: image extracted from the point cloud with colour information (**a**); image with enhanced combining colours and intensity (**b**); morphology obtained by the inclination of the normal direction with respect to a local plane by interpolating the neighbourhood points by 2 cm (**c**).

Figure 9. Fresco of Perseus and Medusa on the vault of the Lodge of Galatea investigated through laser scanning: image extracted from the point cloud with colour information (**a**); image with enhanced combining colours and intensity (**b**); morphology obtained by the inclination of the normal direction with respect to a local plane by interpolating the neighbourhood points by 2 cm (**c**).

The crack pattern can be clearly detected by the laser scanning investigation, although the same frescoes have undergone several restoration interventions over time, which aimed to reduce unwanted visual effects and consolidate the paintings themselves.

Longer cracks in the plaster are detectable:

- On the fresco of Elice, in which from the oxtail it crosses the same decorative space, also affecting the frames (box II of Figure 8a, with detail in Figure 10(II)).
- At the height of the feet of Fame in the fresco of Perseus and Medusa (box I of Figure 9a, with detail in Figure 11(I)), which almost entirely crosses the entire vault transversely.

Moreover, some other local cracks can be identified on the frescoes, e.g., those shown in the box III of Figure 8a, with detail in Figure 10(III), and in the box III of Figure 9a, with detail in Figure 11(III).

In the same way, alterations of the plaster were detectable through the figures, e.g., those shown in the box I of Figure 8a, with detail in Figure 10(I), and in the box II of Figure 9a, with detail in Figure 11(II). It is worth noting that in the first case, there was a rethinking of the author; in fact, the forearm and the hand holding the reins of the oxen seem to be more tense, or in any case in a less-soft position (cf. Figure 10(I)).

By visual inspection of the entire vault, the system of the main cracks has been drawn (Figure 12). The propagation direction of the cracks is mainly along the lower side of the structural element, with an extension from about 49 cm up to 545 cm almost seamlessly and a variable width up to several millimetres. The longest crack is the one that crosses the fresco of Perseus and Medea, already shown also in the previous figure. Moreover, some cracks can also be detected in an orthogonal direction to the previous one, such as the one that rests on the fresco of Elice.

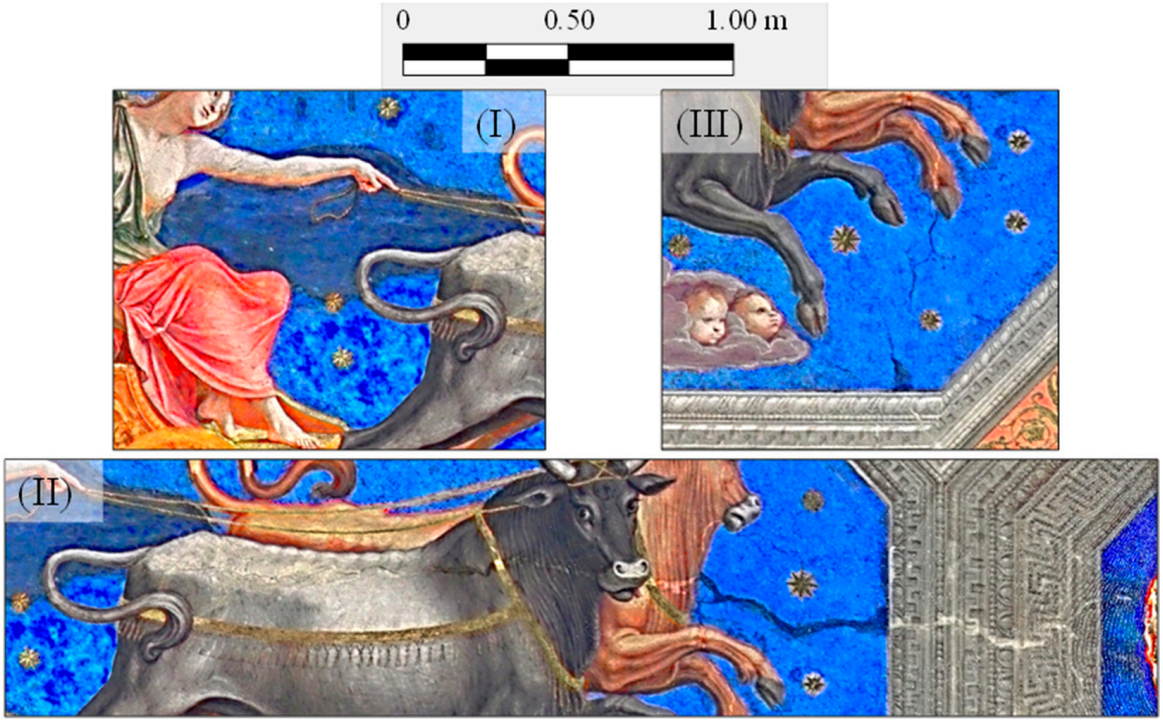

Figure 10. Fresco of Elice on the vault of the Lodge of Galatea investigated through laser scanning: details in terms of colours enhanced by intensity. The subfigures (**I**), (**II**) and (**III**) represent details of the fresco in correspondence of the panels numbered in the same way in Figure 8.

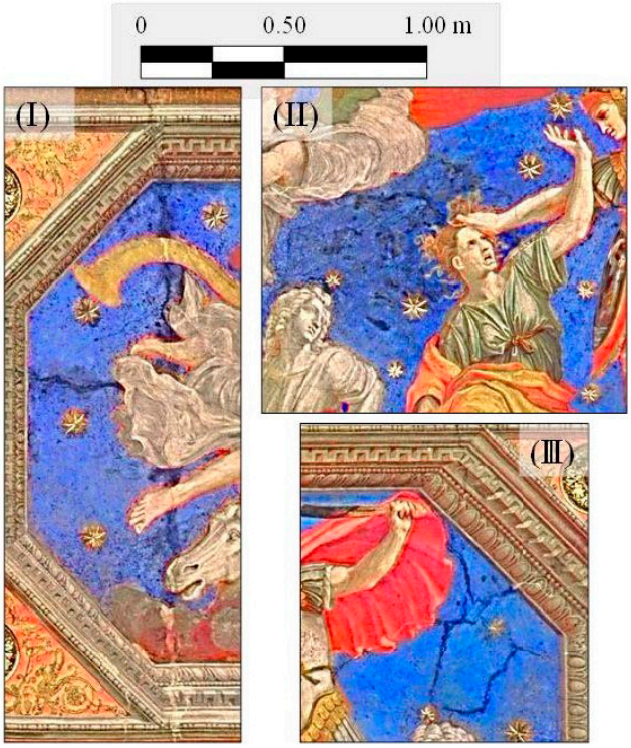

Figure 11. Fresco of Perseus and Medusa on the vault of the Lodge of Galatea investigated through laser scanning: details in terms of colours enhanced by intensity. The subfigures (**I**), (**II**) and (**III**) represent details of the fresco in correspondence of the panels numbered in the same way in Figure 9.

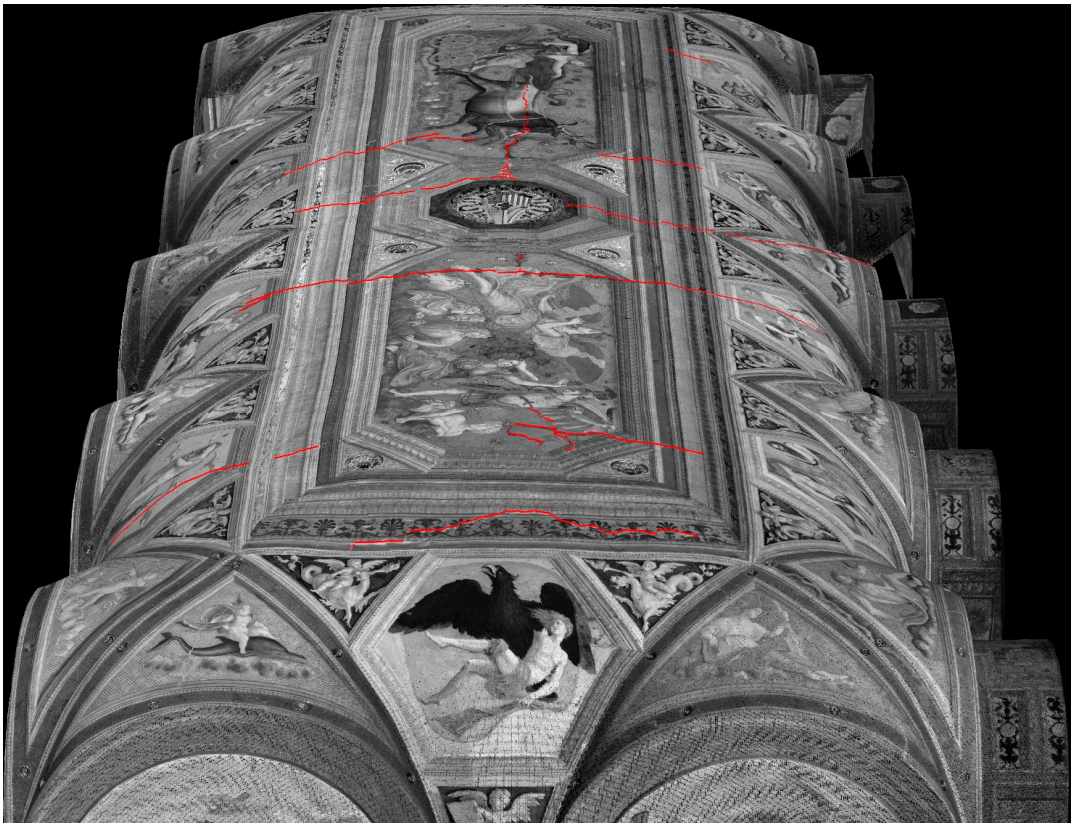

Figure 12. Perspective views of the vault with the main cracks (red traces) detected by inspection of the point clouds.

3.2. The Current Level of the Vibrations

The traffic-induced vibrations were processed both in frequency and time domains, both to describe how the energy is distributed with respect to the frequency content and the to assess maximum values recorded inside and outside the building. The PSDs were obtained by processing the 24 h recorded signals through 250 s-length time windows in the range 0.2–50 Hz (with 256 frequency steps in logarithmic scale), then the mean values and standard deviations were calculated on a typical daily recording during the monitoring period. It is worth highlighting that this observation period was performed during lockdowns and re-openings that had been imposed by the Italian government to tackle the pandemic. Therefore, although the results, which are shown below, were obtained by processing the recordings on 26th October 2020, in which road traffic was allowed throughout the whole day, there may be differences with the pre-pandemic conditions.

The power spectral densities (PSDs) as a function of the frequency obtained by recordings at the ground level are reported in Figure 13. The environment vibration at the garden site on the Lungara side, which is in a restricted traffic area for most of the day, shows only relative PSD peaks at high frequencies (T1186 in Figure 13), both on horizontal and vertical components. Conversely, relevant peaks were encountered at frequencies greater than 10 Hz when analysing recordings at the garden site on the Lungotevere side (T1184 in Figure 13), which are strongly related to the traffic. Thus, the relevant observed variation of the PSD values at higher frequencies is mainly due to the differences during the 24 h between the busiest daytime hours and those at night with less intense traffic (cf. Figure 14). The figure, representing the noise in dB over a time of 72 continuous hours, shows a persistent road load throughout the day, which only significant decreases from 10 p.m. to 4 a.m.

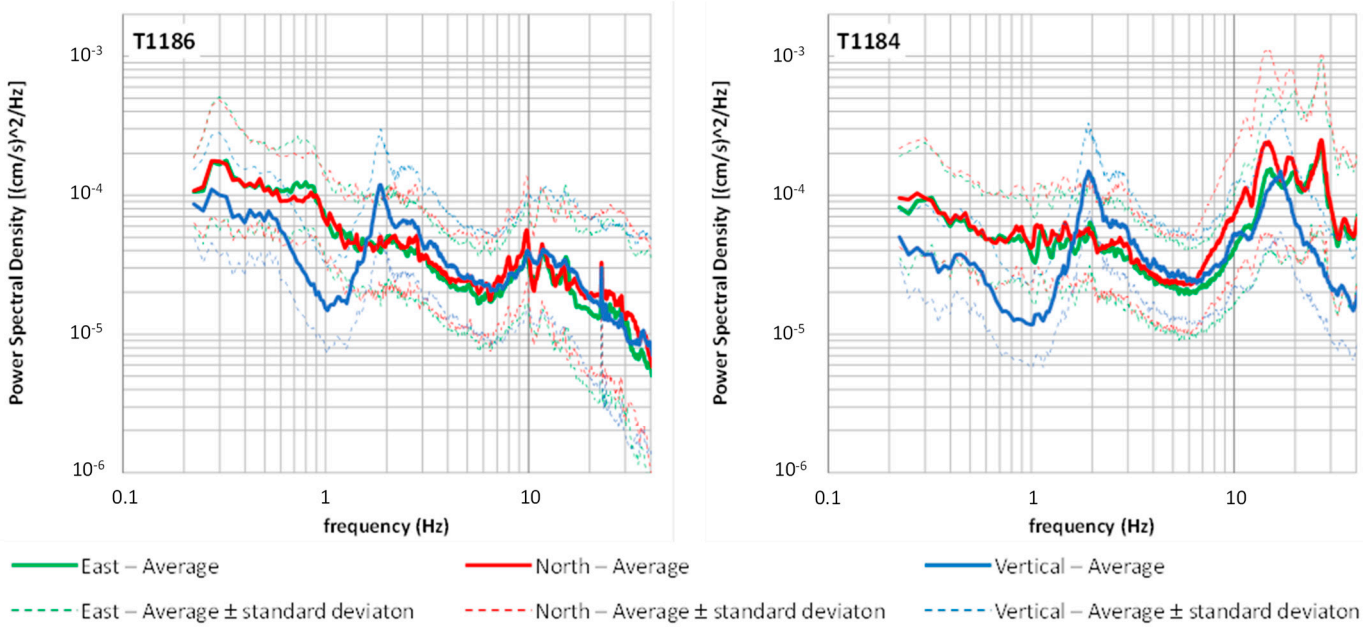

Figure 13. Power spectral densities calculated from the 24 h recordings acquired by the seismic stations in the garden: both on the Lungara (T1186) and Lungotevere (T1184) side.

It is worth also noting that Figure 13 shows a peak around 2 Hz for the vertical component in both sites, and in all other recordings inside the building, with comparable values everywhere. Some authors [14] suggest that this peak is due to the vibration of the embankment of the Tiber River; however, specific monitoring will be performed to confirm it.

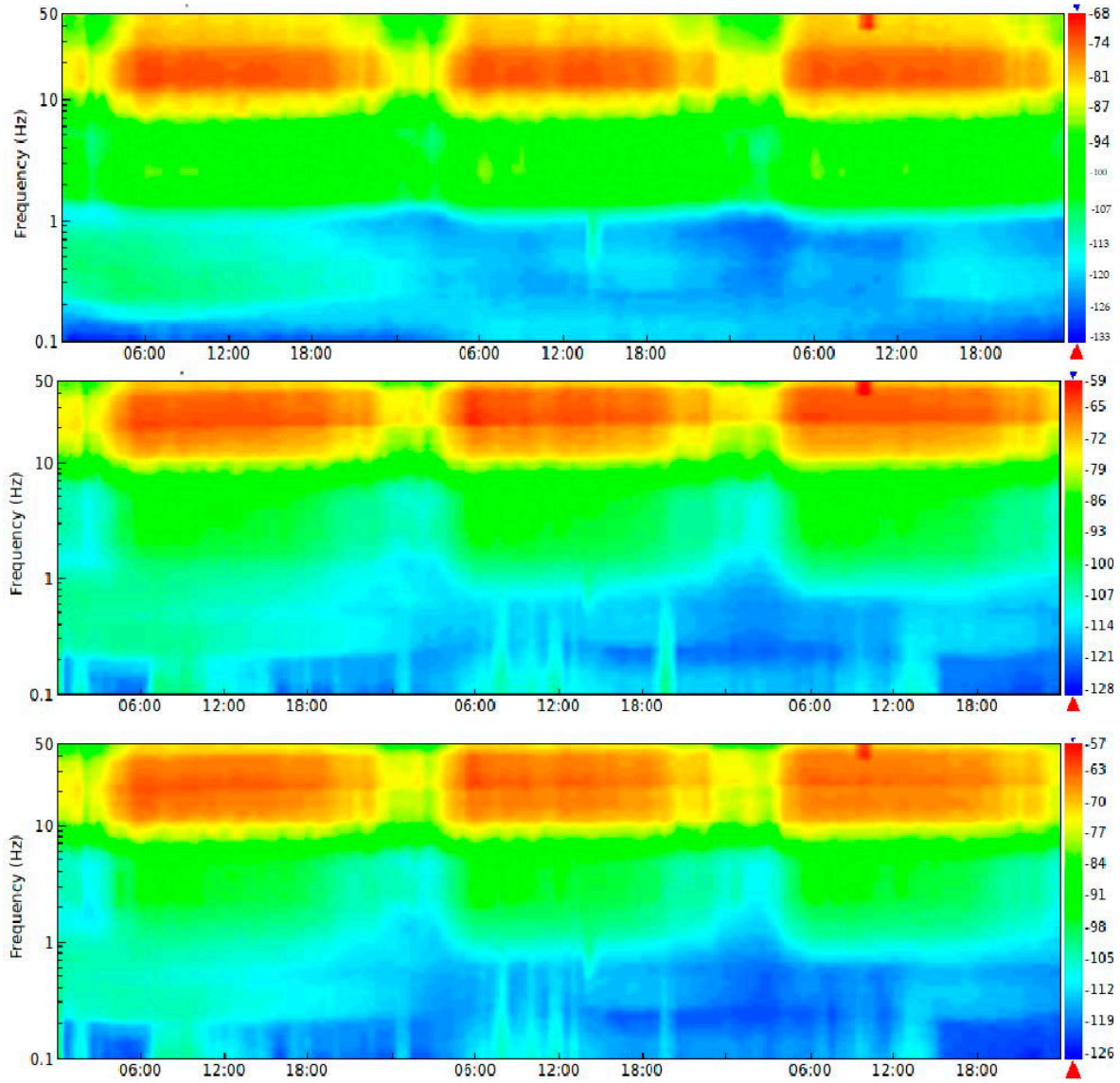

Figure 14. Noise levels expressed in dB as a function of frequency during three recording days, which show the differences between day and night hours at the site in the garden on the Lungotevere side.

Figure 15 shows the ratios between the mean values of the PSDs obtained at the various locations inside and outside the Villa with respect to those in the basement (T1192), which was assumed as the reference site. The ratios are reported for both the vertical and horizontal components, the latter obtained using the geometric mean values of the two components. The vertical components show, for almost all the monitoring sites inside the Villa, a ratio close to or lower than one in the frequency range between 10 Hz and 30 Hz, which is the characteristic frequency range for the traffic load, because the basement on the Lungotevere side is still affected by the vibrations induced by the road traffic. In fact, the decreasing of the ratio at high frequencies is more and more evident moving towards the Lungara side (from red to blue curves in Figure 15a,b). Even so, it is possible to verify this phenomenon by comparing the vertical components of the two sites in the garden, while the one on the Lungotevere side shows a ratio that significantly increases with the frequency from 10 Hz onwards (black curve in Figure 15c); on the other side, there is a value of the ratio that is close to or lower than one in the range between 10 and 20 Hz, which then increases for higher frequencies (grey curve in Figure 15c).

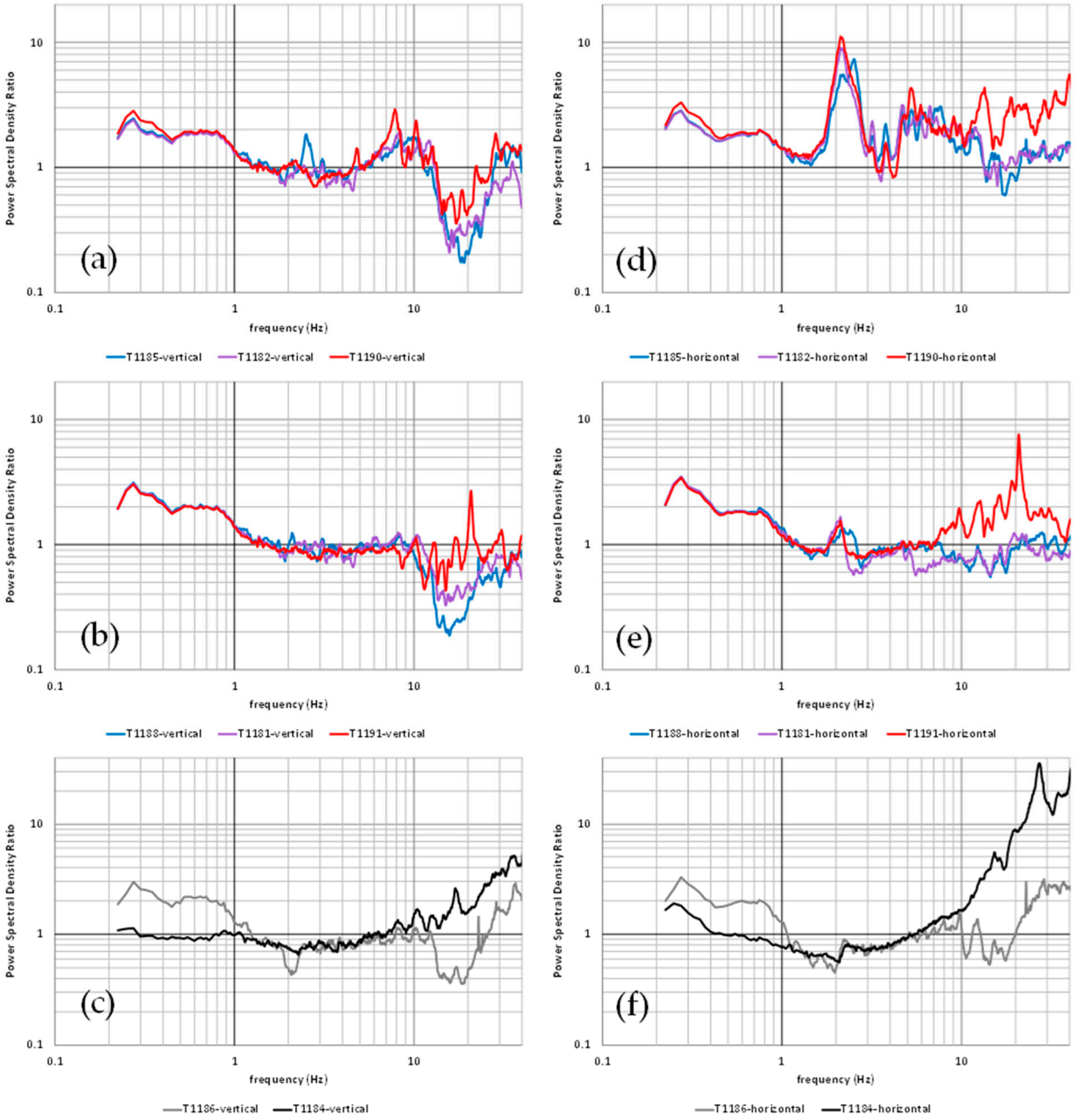

Figure 15. Ratios between the mean values of the PSD calculated at the different recording sites (inside and outside the Villa Farnesina) and those in the basement on the Lungotevere side used as a reference. Ratios for vertical components related to the sites: on the 2nd floor (**a**); on the 1st floor (**b**); in the garden (**c**). Ratios for the mean horizontal components related to the sites: on the 2nd floor (**d**); on the 1st floor (**e**); in the garden (**f**). By analysing one-day time histories, the dynamic identification of the Villa was performed with the Frequency Domain Decomposition (FDD) [52,53] to assess the natural frequencies related to the structural modes (Figure 16a). Figure 16b shows the normalised first singular values with several peaks below 10 Hz, which can be considered as resonant frequencies of the ancient building. As already shown in the previous figures and in other works (e.g., [13,14]), the traffic noise has a clear effect on frequencies greater than about 10 Hz; therefore, this behaviour hides the resonant peaks at the higher frequencies. Nevertheless, the FDD analysis, even if the white noise input assumption is not satisfied, allows estimating the first frequencies and the related damping ratios due to the structural modes (Figure 16b and Table 2).

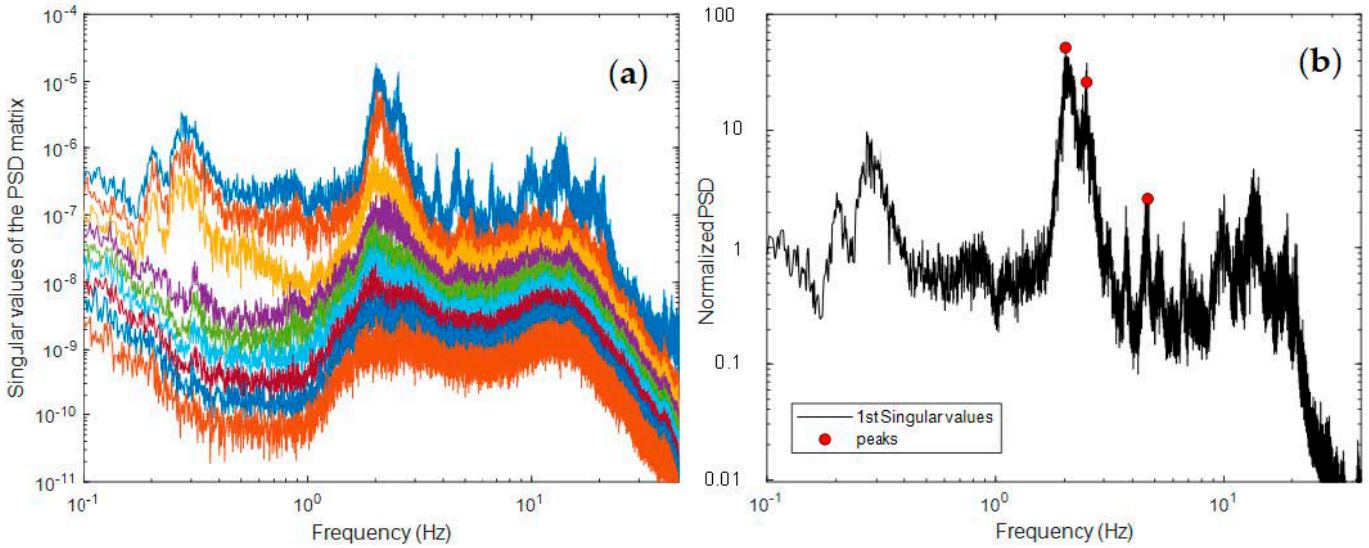

Figure 16. Singular value decomposition (SVD) of the power spectral density (PSD) matrix (**a**) and normalised 1st singular values (**b**), with the red circles identifying peaks corresponding to the structural modes lower than about 10 Hz.

Table 2. Structural modes of the ancient building below about 10 Hz.

Structural Modes	1	2	3
Natural frequency [Hz]	2.016	2.522	4.651
Damping ratio [%]	4.07	4.08	2.78

The horizontal components of the ratio show values significantly greater than one, highlighted only for the recording sites on the Lungotevere side at the upper levels (red curves in Figure 15d,e). It is worth noting that the same horizontal components allow identifying two resonance peaks in the range between 2.0 Hz and 2.7 Hz (Figure 15d), which are linked to the vibration modes of the building. Similar to what was discussed for the vertical components, the PSD amplitudes are much greater than those of the basement on the Lungotevere side above 10 Hz, whereas, at the garden site on the Lungara side, the ratio is (or is close to) less than one between 10 Hz and 20 Hz, then increases at higher frequencies (Figure 15f).

Moreover, the particle motions for the inside and outside locations close to the Lungotevere road were obtained from the velocity time-histories, filtered with a rectangular band-pass filter in the range between 10 and 50 Hz. The motions on the horizontal east–north plane (Figure 17a) and on the vertical ones (north–vertical in Figure 17b and east–vertical in Figure 17c) show that the Peak Particle Velocity (PPV) is always lower than 2 mm/s. In fact, the PPV assumes a maximum value of about 1.4 mm/s (and maximum Peak Particle Velocity—PCPV of 1.1 mm/s) considering all the three components recorded on the second floor of the Villa; instead, it assumes much smaller values on the lower floors. It has been noted that choosing different filter shapes to apply to the time history produces slight differences in the maximum values in the time domain.

The predominant horizontal direction from the recordings within the Villa (between 50 and 55°N clockwise) is almost orthogonal to the stretch of the road axis (about 137°N clockwise); instead, it is less defined from the recordings outside the Villa, and has with a predominant direction characterised by smaller angles with respect to the north (Figure 17a). At the same time, the maximum velocities on the vertical component of the motion in the range 10–50 Hz appears negligible in the garden; instead, they assume maximum values almost comparable to the horizontal ones from the recordings inside the building (Figure 17b,c).

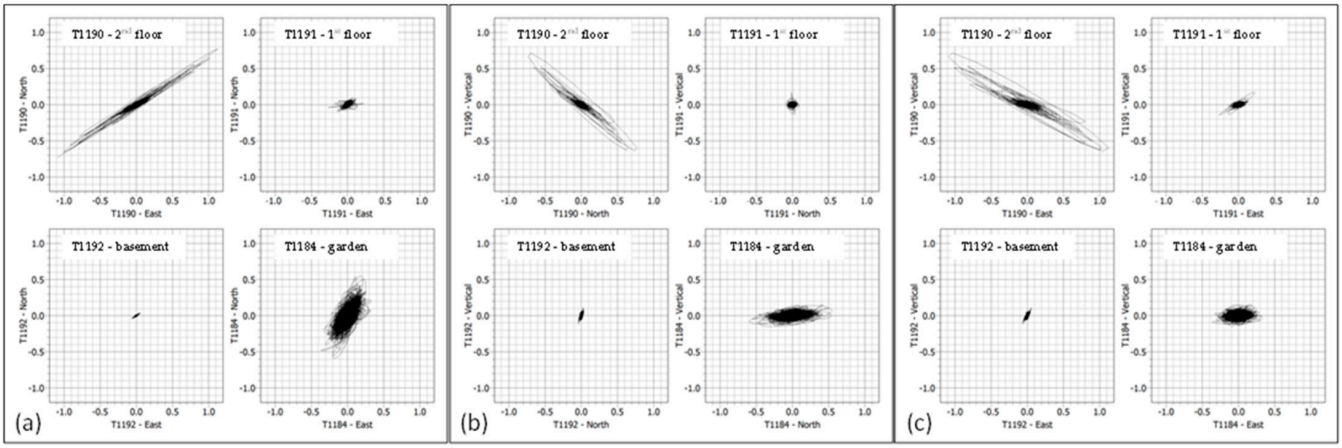

Figure 17. Particle velocity in mm/s at the recording sites on the Lungotevere side (both inside and outside the Villa Farnesina) on the east–north horizontal (**a**), north–vertical (**b**) and east–vertical plane (**c**).

4. Discussion

As for the preliminary survey obtained on the lodge of Galatea in the Villa Farnesina, the inspection through the laser scanning technique shows open cracks even of several millimetres. Moreover, often the width of the altered plaster in the surrounding of the cracks appears more consistent, even with a width for an order of magnitude greater than that of the fracture. This appears evident on some parts of the frescoes on the vault by comparing local morphological anomalies, which highlight damage due only to geometric anomalies, as well as by analysing the reflectance intensities combined with colours, which show a wider alteration, producing differences in the laser signal up to some centimetres, with respect to the material conditions around the crack. Moreover, some material alterations can be also detectable in other portions of the frescoes, where relevant cracks do not appear. It is worth underlining that some of these material anomalies could also be the result of restoration works that aimed to repair the damage that had occurred in the past. However, a further investigation on the historical sources regarding the restoration interventions could support these considerations in future developments of this research work, and useful information can be provided by the comparison between the laser scanning acquisitions shown in the paper and those that will be obtained after the last restoration work carried out in recent months on the same lodge.

The geophysical monitoring showed vibration levels lower than the threshold values suggested by international standards to trigger effects on the assets. This, on the one hand, seems to prove a certain effectiveness of interventions to improve the road infrastructure, which is the main local source of vibrations for frequencies around (and greater) than 10 Hz. However, even today the vibrations are still not negligible, and therefore could be capable of producing negative effects on the frescoed paintings, for which even cracks of a few millimetres can produce a loss of the aesthetic value, without considering the costs of their restoration. Moreover, it is worth pointing out that the recordings were acquired at the turn of the lockdown periods due to the COVID-19 pandemic in Italy, so the vibration levels are probably underestimated compared to the previous period.

Most major cracks are in the middle part of the vault along its longer side, and their propagation direction is practically along the transversal direction of the vault, therefore about 10–15° clockwise with respect to the predominant direction of the particle motion on the horizontal plane. Moreover, some other relevant cracks also have developed along the longer side of the vault.

5. Conclusions

The vibrations induced by traffic loads are one of the most important causes of aesthetic damages on the cultural heritage assets (buildings and artefacts) and archaeological sites, especially those located close to or within urban areas. Although national and international standards establish threshold limits of vibration not to be exceeded to ensure that this does not affect the cultural heritage assets, often these limits are characterised by different procedures, range frequencies and threshold values. It is also worth highlighting that the processing of experimental data can influence the results to be compared with the thresholds, not only when accelerometers are used in the survey campaign, and therefore it is necessary to integrate the recordings [13], for example, by optimising the choice of the filtering method to process time-histories in a specific frequency range. Moreover, the suggested damage thresholds do not provide safety [54], but they are only indicative, and these limits do not consider the current health state of the cultural heritage assets.

In this context, the purpose of the paper was to show a combined use of proximal remote sensing and geophysical monitoring on the real case represented by Villa Farnesina in Rome, both to retrieve information for a better knowledge of the health state of the assets and to assess the vibration levels to which they are subject, as both are essential to assess the risk level. In fact, the building and its Renaissance masterpieces have already suffered damage because of the environmental vibrations due to human activities that have been more or less prolonged over time, as reported by testimonies and technical reports in the past.

Preliminarily, a first investigation carried out by laser scanning on the Lodge of Galatea allowed the detection of the crack pattern and the plaster deterioration in the most exposed elements of the building in its part closest to the Lungotevere, which is represented by the frescoes on the vault. The findings have highlighted important cracks on the frescoes investigated, although these have been the subject of restorations over time, which are indicative of a significant vulnerability. The high-resolution point clouds obtained through laser scanning will make it possible to have a reference for comparative analyses following periodic future surveys (both using visual inspection or automated algorithms—e.g., [55–59]), the first of which will be planned in the coming months after the end of the last restoration activities carried out on the lodge itself.

Geophysical monitoring, on the other hand, highlighted values of vibrations below the thresholds suggested by national and international codes to produce effects on cultural heritage. However, the high vulnerability shown in the past, with the effects still detectable today, and the non-negligible level of environmental vibrations, suggest continuing to keep the Villa Farnesina under observation, as well as continuing to assess the direct connection between vibrations induced by traffic (and any other human activities or natural event) and the onset of negative effects on the frescoes.

With this purpose, the National Institute of Geophysics and Volcanology and the Accademia dei Linceii are studying solutions to start a permanent and continuous monitoring system in the near future to verify any variations in the vibrational regime in near real time, thus allowing the planning of any necessary interventions. In addition, in these future developments, the implementation also of periodic monitoring based on non-destructive techniques (e.g., terrestrial radar interferometry, ultrasonic tests, image-based approaches) will also be evaluated, in order to study the vibration modes of single elements of interest, structural and non-structural, in the historic building, as well as evaluate the onset of further aesthetic damage on the assets. Furthermore, a long-term monitoring of vibrations and the state of the surfaces of the asset, with the techniques presented as well as with the addition of other new ones, could allow us to link the vibration levels to the detectable effects.

Author Contributions: Conceptualization, A.C., M.F.B., M.M., A.S., V.L.; methodology, A.C.; formal analysis, A.C.; investigation, A.C., M.M., S.F., C.L.P.; resources, A.C., A.S. and V.L.; data curation, A.C., S.F., C.L.P.; writing—original draft preparation, A.C., M.M.; writing—review and editing, A.C.; supervision, A.C.; project administration, A.C., M.F.B.; funding acquisition, M.F.B. All authors have read and agreed to the published version of the manuscript.

Funding: This research was funded by INGV in the framework of the Project MIUR 2020–2029 Pianeta Dinamico: Geoscienze per la comprensione dei meccanismi di funzionamento della Terra e dei conseguenti rischi naturali—Working Earth: geosciences and understanding of the earth dynamics and natural hazards" (CUP D53J19000170001).

Data Availability Statement: The data presented in this study are available on request from the corresponding author.

Acknowledgments: The authors thank the Accademia dei Lincei and the staff of the Villa Farnesina for supporting the installation phase of the monitoring system. In addition, the authors would like to thank the reviewers and the academic editor for their valuable comments which helped improve the article.

Conflicts of Interest: The authors declare no conflict of interest.

References

1. Tatì, M.B.; Cianetti, M.M.; de Canio, G.E. Impact of traffic vibration on the temple of Minerva Medica, Rome: Preliminary study within the co.b.ra. project. *Int. J. Herit. Archit. Stud. Repairs Maintence* **2017**, *2*, 102–114. [CrossRef]
2. Giovanis, E. The relationship between teleworking, traffic and air pollution. *Atmos. Pollut. Res.* **2018**, *9*, 1–14. [CrossRef]
3. Guo, Y.; Zhang, Q.; Lai, K.K.; Zhang, Y.; Wang, S.; Zhang, W. The Impact of Urban Transportation Infrastructure on Air Quality. *Sustainability* **2020**, *12*, 5626. [CrossRef]
4. Betta, L.; Dattilo, B.; di Bella, E.; Finocchiaro, G.; Iaccarino, S. Tourism and Road Transport Emissions in Italy. *Sustainability* **2021**, *13*, 12712. [CrossRef]
5. Rainer, J.H. Effect of vibrations on historic buildings: An overview. *Assoc. Preserv. Technol. Bull.* **1982**, *15*, 2–10. [CrossRef]
6. Xia, B.; Wei, P.B.; Cao, Y.M. Traffic-induced vibrations of ground environments and buildings. In *Environmental Vibrations: Prediction, Monitoring, Mitigation and Evaluation*, 1st ed.; Takemiya, H., Ed.; Taylor & Francis Group: London, UK, 2005; pp. 529–539.
7. Beben, D.; Maleska, T.; Bobra, P.; Duda, J.; Anigacz, W. Influence of Traffic-Induced Vibrations on Humans and Residential Building-A Case Study. *Int. J. Environ. Res. Public Health* **2022**, *19*, 5441. [CrossRef]
8. Caserta, A.; Doumaz, F.; Costanzo, A.; Gervasi, A.; Thorossian, W.; Falcone, S.; La Piana, C.; Minasi, M.; Buongiorno, M.F. Assessing soil-structure interaction during the 2016 central Italy seismic sequence (Italy): Preliminary results. *Ann. Geophys.* **2016**, *59*, 1–7.
9. Costanzo, A.; Caserta, A. Seismic response across the Tronto Valley (at Acquasanta Terme, AP, Marche) based on the geophysical monitoring of the 2016 Central Italy seismic sequence. *Bull. Eng. Geol. Environ.* **2019**, *78*, 5599–5616. [CrossRef]
10. Costanzo, A.; D'Onofrio, A.; Silvestri, F. Seismic response of a geological, historical and architectural site: The Gerace cliff (southern Italy). *Bull. Eng. Geol. Environ.* **2019**, *78*, 5617–5633. [CrossRef]
11. Ferraro, A.; Grasso, S.; Maugeri, M.; Totani, F. Seismic response analysis in the southern part of the historic centre of the City of L'Aquila (Italy). *Soil Dyn. Earthq. Eng.* **2016**, *88*, 256–264. [CrossRef]
12. Brando, G.; Pagliaroli, A.; Cocco, G.; Di Buccio, F. Site effects and damage scenarios: The case study of two historic centers following the 2016 Central Italy earthquake. *Eng. Geol.* **2020**, *272*, 105647. [CrossRef]
13. Zini, G.; Betti, M.; Bartoli, G. Experimental analysis of the traffic-induced-vibration on an ancient lodge. *Struct. Control Health Monit.* **2022**, *29*, e2900. [CrossRef]
14. Clemente, P.; Rinaldis, D. Protection of a monumental building against traffic-induced vibrations. Soil Dyn. *Earthq. Eng.* **1998**, *17*, 289–296. [CrossRef]
15. Korkmaz, K.A.; Ay, Z.; Keskin, S.N.; Ceditoglu, D. Investigation of traffic-induced vibrations on masonry buildings in Turkey and countermeasures. *J. Vib. Control* **2011**, *17*, 3–10. [CrossRef]
16. Baraccani, S.; Azzara, R.M.; Palermo, M.; Gasparini, G.; Trombetti, T. Long-term seismometric monitoring of the two towers of bologna(Italy): Modal frequencies identification and effects due to traffic induced vibrations. *Front. Built Environ.* **2020**, *6*, 85. [CrossRef]
17. Haladin, I.; Bogut, M.; Lakušić, S. Analysis of Tram Traffic-Induced Vibration Influence on Earthquake Damaged Buildings. *Buildings* **2021**, *11*, 590. [CrossRef]
18. Persson, P.; Andersen, L.V.; Persson, K.; Bucinskas, P. Effect of structural design on traffic-induced building vibrations. *Procedia Eng.* **2017**, *199*, 2711–2716. [CrossRef]
19. Pau, A.; Vestroni, F. Vibration assessment and structural monitoring of the Basilica of Maxentius in Rome. *Mech. Syst. Signal Process.* **2013**, *41*, 454–466. [CrossRef]

20. Crispino, M.; D'Apuzzo, M. Measurement and prediction of traffic-induced vibrations in a heritage building. *J. Sound Vib.* **2001**, *246*, 319–335. [CrossRef]
21. Erkal, A. Transmission of Traffic-induced Vibrations on and around the Minaret of Little Hagia Sophia. *Int. J. Archit. Herit.* **2017**, *11*, 349–362. [CrossRef]
22. Lorenzoni, F.; Casarin, F.; Modena, C.; Caldon, M.; Islami, K.; da Porto, F. Structural health monitoring of the Roman Arena of Verona, Italy. *J. Civ. Struct. Health Monit.* **2013**, *3*, 227–246. [CrossRef]
23. Puzzilli, L.M.; Bongiovanni, G.; Clemente, P.; Di Fiore, V.; Verrubbi, V. Effects of Anthropic and Ambient Vibrations on Archaeological Sites: The Case of the Circus Maximus in Rome. *Geosciences* **2021**, *11*, 463. [CrossRef]
24. Bernardini, G.; De Pasquale, G.; Gallino, N.; Gentile, C. Microwave interferometer for ambient vibration measurements on civil engineering structures: 2. Application to full-scale Bridges. In Proceedings of the Experimental Vibration Analysis for Civil Engineering Structures (EVACES'07), Porto, Portugal, 24–26 October 2007; pp. 153–162.
25. Mugnai, F.; Cosentino, A.; Mazzanti, P.; Tucci, G. Vibration Analyses of a Gantry Structure by Mobile Phone Digital Image Correlation and Interferometric Radar. *Geomatics* **2022**, *2*, 17–35. [CrossRef]
26. Antonielli, B.; Caporossi, P.; Mazzanti, P.; Moretto, S.; Rocca, A. InSAR & Photomonitoringtm for Dams and Reservoir Slopes Health & Safety Monitoring. In Proceedings of the Twenty-Sixth International Congress on Large Dams/Vingt-Sixième Congrès International des Grands Barrages, Vienna, Austria, 4–6 July 2018; p. 4.
27. Mugnai, F.; Tucci, G.; Da Re, A. Digital image correlation in assessing structured-light 3D scanner's gantry stability: Performing david's (michelangelo) high-accuracy 3D survey. In Proceedings of the International Archives of the Photogrammetry, Remote Sensing and Spatial Information Sciences, Torino, Italy, 1 August 2021; Volume XLVI-M-1–2, pp. 463–469.
28. Ozelim, L.C.d.S.M.; Borges, L.P.d.F.; Cavalcante, A.L.B.; Albuquerque, E.A.C.; Diniz, M.d.S.; Góis, M.S.; Costa, K.R.C.B.d.; Sousa, P.F.d.; Dantas, A.P.d.N.; Jorge, R.M.; et al. Structural Health Monitoring of Dams Based on Acoustic Monitoring, Deep Neural Networks, Fuzzy Logic and a CUSUM Control Algorithm. *Sensors* **2022**, *22*, 2482. [CrossRef] [PubMed]
29. *DIN 4150-3:1999*; Structural Vibrations—Part 3: Effects of Vibration on Structures. Deutsches Institut fur Normung: Berlin, Germany, 2016.
30. *UNI 9916:2014*; Criteri di Misura e Valutazione Degli Effetti Delle Vibrazioni Sugli Edifici. Ente Nazionale Italiano di Unificazione: Milan, Italy, 2014.
31. *SN 640312:2013*; Effet des Ébranlements sur les Constructions. Swiss Standard: Swiss, Switzerland, 2013.
32. UNESCO World Heritage List. Available online: https://whc.unesco.org/en/list/ (accessed on 21 April 2021).
33. Villa Farnesina: A Resilience Laboratory. Traffic Vibrations: The project by Prof. Eng. Gustavo Colonnetti, Lincei Fellow (1886–1968). Accademia dei Lincei, Roma. Available online: http://www.Villafarnesina.it/wp-content/uploads/2020/12/TotemTraffico3.pdf (accessed on 21 May 2022).
34. INGV Project Dynamic Planet. Available online: https://progetti.ingv.it/en/pianeta-dinamico (accessed on 21 April 2021).
35. Costanzo, A.; Falcone, S.; La Piana, C.; Lapenta, V.; Musacchio, M.; Sgamellotti, A.; Buongiorno, M.F. Traffic-induced vibrations on cultural heritage in urban area: The case of Villa Farnesina in Rome. *J. Phys. Conf. Ser.* **2022**, *2204*, 012043. [CrossRef]
36. Colonnetti, G.; Massari, G. *Relazione per lo Studio dei Danni Arrecati dal Traffico Pesante alla Farnesina*; Accademia Nazionale dei Lincei: Roma, Italy, 1959. (In Italian)
37. Pfeifer, N.; Briese, C. Laser scanning: Principles and applications. In Proceedings of the 3rd International Exhibition and Scientific Congress on Geodesy, Mapping, Geology, Geophysics, Novosibirsk, Russia, 25–27 April 2007.
38. Andrews, D.D.; Bedford, J.; Papworth, H. *; English Heritage. Measured and Drawn: Techniques and Practice for the Metric Survey of Historic Buildings*; English Heritage: Swindon, UK, 2009.
39. Z+F IMAGER®5010C. Available online: https://www.zofre.de/en/laser-scanners/3d-laser-scanner/z-f-imagerr-5010c (accessed on 2 July 2022).
40. Olsen, M.J.; Kuester, F.; Chang, B.J.; Hutchinson, T.C. Terrestrial laser scanning-based structural damage assessment. *J. Comput. Civ. Eng.* **2010**, *24*, 264–272. [CrossRef]
41. Costanzo, A.; Minasi, M.; Casula, G.; Musacchio, M.; Buongiorno, M.F. Combined Use of Terrestrial Laser Scanning and IR Thermography Applied to a Historical Building. *Sensors* **2015**, *15*, 194–213. [CrossRef]
42. Costanzo, A.; Pisciotta, A.; Pannaccione Apa, M.I.; Bongiovanni, S.; Capizzi, P.; D'Alessandro, A.; Martorana, R. Integrated use of unmanned aerial vehicle photogrammetry and terrestrial laser scanning to support archaeological analysis: The Acropolis of Selinunte case (Sicily, Italy). *Archaeol. Prospect.* **2020**, *28*, 153–165. [CrossRef]
43. Z+F LaserControl®. Available online: https://www.zofre.de/en/laser-scanners/laserscanning-software/z-f-lasercontrolr (accessed on 2 July 2022).
44. Cloud Compare Documentation. Available online: https://www.cloudcompare.org/doc/wiki/index.php/Main_Page (accessed on 2 July 2022).
45. Gillespie, A.R.; Kahle, A.B.; Walker, R.E. Color enhancement of highly correlated images-II: Channel ratio and "chromaticity" transformation techniques. *Remote Sens. Environ.* **1987**, *22*, 343–365. [CrossRef]
46. Nanometrics Inc. *CENTAUR Technical Specifications*; Nanometrics, Inc.: Kanata, ON, Canada, 2018. Available online: https://www.nanometrics.ca/products/digitizers/centaur-digital-recorder (accessed on 2 July 2022).
47. Nanometrics Inc. *TRILLIUM COMPACT Technical Specifications*; Nanometrics, Inc.: Kanata, ON, Canada, 2018. Available online: https://www.nanometrics.ca/products/seismometers/trillium-compact (accessed on 2 July 2022).

48. Nanometrics Inc. *TITAN Technical Specifications*; Nanometrics, Inc.: Kanata, ON, Canada, 2018. Available online: https://www.nanometrics.ca/products/accelerometers/titan-accelerometer (accessed on 2 July 2022).
49. McNamara, D.E.; Buland, R.P. Ambient Noise Levels in the Continental United States. *Bull. Seism. Soc. Am.* **2004**, *94*, 1517–1527. [CrossRef]
50. PQLX Software. Available online: https://ds.iris.edu/ds/nodes/dmc/software/downloads/pqlx/2011365p4/ (accessed on 2 July 2022).
51. Peterson, J. *Observations and Modeling of Seismic Background Noise*; US Geological Survey Open-File Report; US Geological Survey: Reston, VA, USA, 1993; pp. 93–322.
52. Brincker, R.; Zhang, L.; Andersen, P. Modal Identification from Ambient Responses using Frequency Domain Decomposition. In Proceedings of the International Modal Analysis Conference (IMAC), San Antonio, TX, USA, 7–10 February 2000; pp. 625–630.
53. Brincker, R.; Zhang, L.; Andersen, P. Modal identification of output-only systems using frequency domain decomposition. *Smart Mater. Struct.* **2001**, *10*, 441. [CrossRef]
54. Athanasopuolos, G.A.; Pelekis, P.C. Ground vibrations from sheetpile driving in urban environment: Measurements, analysis and effects on buildings and occupants. *Soil Dyn. Earthq. Eng.* **2000**, *19*, 371–387. [CrossRef]
55. Lague, D.; Brodu, N.; Leroux, J. Accurate 3D comparison of complex topography with terrestrial laser scanner: Application to the Rangitikei canyon (N-Z). *ISPRS J. Photogramm. Remote Sens.* **2013**, *82*, 10–26. [CrossRef]
56. Lercari, N. Monitoring earthen archaeological heritage using multi-temporal terrestrial laser scanning and surface change detection. *J. Cult. Herit.* **2019**, *39*, 152–165. [CrossRef]
57. Barnhart, T.B.; Crosby, B.T. Comparing Two Methods of Surface Change Detection on an Evolving Thermokarst Using High-Temporal-Frequency Terrestrial Laser Scanning, Selawik River, Alaska. *Remote Sens.* **2013**, *5*, 2813–2837. [CrossRef]
58. Yang, H.; Xu, X. Intelligent crack extraction based on terrestrial laser scanning measurement. *Meas. Control* **2020**, *53*, 3–4. [CrossRef]
59. Stałowska, P.; Suchocki, C.; Rutkowska, M. Crack detection in building walls based on geometric and radiometric point cloud information. *Autom. Constr.* **2022**, *134*, 104065. [CrossRef]